SUPPLEMENTAL MATERIALS

SUPPLEMENTAL METHODS

Human subjects. A total of 38 patients with systemic lupus erythematosus (SLE) were investigated. All patients satisfied the criteria for a definitive diagnosis [1;2]. Disease activity was assessed by SLEDAI score [3]. Seventeen patients were treated with rapamycin with therapeutic target of plasma concentrations at 6-15 ng/ml (mean age: 38.6 ± 15 years, ranging between 21-65 years; SLEDAI: 6.9 ± 3.7). 15 patients were Caucasian females, 1 patient was Caucasian male, and 1 patient was African-American female. Among the 21 remaining SLE patients treated without rapamycin, 10 were receiving prednisone, 10 were receiving mycophenolic acid, 8 were receiving mycophenolate mofetil, 2 were receiving 6-mercaptopurine, 1 was receiving cyclosporin A. Their mean age was 45.4 ± 14 years, ranging between 18-69 years; SLEDAI: 6.7 ± 4.4. As controls, 21 healthy subjects were studied
in parallel, matched for gender, ethnicity, and age of SLE patients for each blood donation. 17 controls were Caucasian females, 3 controls were Caucasian males, and 1 control was African-American female. The study has been approved by the Institutional Review Board for the Protection of Human Subjects.

Separation and culture of human peripheral blood lymphocytes. Peripheral blood mononuclear cells (PBMC) were isolated from heparinized venous blood on Ficoll-Hypaque gradient. Peripheral blood lymphocytes (PBL) were separated from monocytes by adherence to autologous serum-coated Petri dishes [4]. T cells (>95% CD3+) were negatively isolated from PBMC with Dynal magnetic beads conjugated to IgG antibodies for CD14, CD16 HLA class II DR/DP, CD56 and CD235a; Invitrogen Cat No.113-11D). CD4+ T cells (>98% CD4+) were negatively isolated with magnetic beads conjugated to IgG antibodies for CD8, CD14, CD16, HLA class II DR/DP, CD56, CDw123, and CD235a (Invitrogen Cat No.113-39D). The resultant cell population was resuspended at 10^6 cells/ml in RPMI 1640 medium, supplemented with 10% fetal calf serum (FCS), 2 mM L-glutamine, 100 IU/ml penicillin, and 100 µg/ml gentamicin in 12-well plates at 37^{o}C in a humidified atmosphere with 5% CO_2. Cross-linking of the CD3 antigen was performed by addition of cells to plates pre-coated with 100 µg/ml goat anti-mouse IgG (Jackson, West Grove, PA) for 2 h and, after washing, pre-coated with 1 µg/ml OKT3 monoclonal antibody (CRL 8001 from ATCC, Rockville, MD) for 1 h at 37^{o}C. CD28 co-stimulation was performed by addition of 500 ng/ml mAb CD28.2 (Pharmingen, San Diego, CA). In vitro treatments of PBL or negatively isolated T cells was performed with rapamycin (50 nM dissolved in DMSO, Cell Signaling Cat# 9904) and bafilomycin A1, used as a lysomomal inhibitor to facilitate detection of proteins (200 nM; Calbiochem).

Mouse embryonic fibroblasts (MEFs). MEFs deficient in Drp1 [5] were provided by Drs. Katsuyoshi Mihara (Kyushu University) and David Chan (California Institute of Technology) and cultured in DMEM medium supplemented with 10% FBS, 2 mM L-glutamine, 100 U/mL penicillin, 100 µg/mL streptomycin, 10 µg/mL amphotericin B, 1% MEM non-essential amino acid solution (10 mM, InVitrogen), and 1 mM sodium pyruvate [5].

Mice. Female New Zealand White (NZW), New Zealand White x New Zealand Black F1 (NZB/W F1), B6.NZMSle1/Sle2/Sle3, MRL, MRL/lpr, C57BL/6 (B6), and C57BL/6.Lpr (B6/Lpr) mice were obtained from Jackson laboratories (Bar Harbor, ME). Female NZB/W F1 mice and age-matched Balb C/NZW and B6 controls were received from Dr. Ram Singh at

University of California Los Angeles. Animal experimentation has been approved by the Committee on the Human Use of Animals in accordance with NIH Guide for the Care and Use of Laboratory Animals.

Isolation of mouse lymphocyte subsets. The harvested spleen tissue was filtered through a 70-μm cell strainer and splenocytes were recovered in DMEM medium, supplemented with 10% fetal calf serum (FCS), 2 mM L-glutamine, 100 IU/ml penicillin, and 100 μg/ml gentamicin. ACK buffer (0.15 M NH_4Cl, 10mM $KHCO_3$, 1 mM Na_2EDTA) was used for lysing of red blood cells for 5 minutes at room temperature. CD3 T cells (Cat # 114.13D), CD4 T cells (Cat# 11461D), CD8 T cells (Cat# 11462D), and B cells (Cat# 11422D) were isolated with magnetic beads following the manufacturer's instructions (InVitrogen, Carlsbad, CA). Naïve $CD44^{low}CD62L^{high}$ $CD4^+$ T cells were isolated with the EasySep protocol (StemcellTechnologies, Vancouver, BC, Canada; Cat #19765). 85-95% purity of cell separations was confirmed for each isolation by flow cytometry.

Flow cytometric analysis of mitochondrial transmembrane potential ($\Delta\Psi_m$) and mitochondrial mass, and nitric oxide. $\Delta\Psi_m$ was estimated by staining for 15 min at 37°C in the dark with 1 μM TMRM (excitation: 543 nm, emission: 567 nm recorded in FL-2) and 20 nm 3,3'-dihexyloxacarbocyanine iodide ($DiOC_6$, excitation: 488 nm, emission: 525 nm recorded in FL-1). Co-treatment with a protonophore, 5 μM carbonyl cyanide m-chlorophenylhydrazone (mClCCP, Sigma) for 15 min at 37°C resulted in decreased TMRM and $DiOC_6$ fluorescence and served as a positive control for disruption of mitochondrial transmembrane potential [6]. Mitochondrial mass was monitored by staining with 100 nM MitoTracker Green-FM (excitation: 490 nm, emission: 516 nm recorded in FL-1) or 100 nM MitoTracker Deep Red (MTDR, excitation: 644 nm, emission: 665 nm). Production of nitric oxide (NO) was assessed by using 4-amino-5-methylamino-2',7'-difluoroflourescein diacetate (DAF-FM; excitation: 495 nm, emission: 518 nm, recorded in FL-1). Measurement of NO was calibrated by incubating PBL with NO donors NOC-18 (200 μM to 1.8 mM) or sodium nitroprusside (SNP; 400 μM to 10 mM), as earlier described [7]. All above fluorescent probes were obtained from Invitrogen/Molecular Probes (Eugene, OR). Diaminorhodamine-4M was used to evaluate peroxynitrite production (DAR-4M, Calbiochem, San Diego, CA; excitation 544 nm, emission 590 nm). Samples were analyzed using a Becton Dickinson LSRII flow cytometer equipped with 20 mW solid-state Ng-YAG (emission at 355 nm), 20 mW argon (emission at 488 nm), 10 mW diode-pumped solid-state yellow-green (emission at 535 nm), and 16 mW helium-neon lasers (emission at 634 nm). Data were analyzed with Flow Jo software (TreeStar Corporation, Ashland, OR). Dead cells and debris were excluded from the analysis by electronic gating of forward (FSC) and side scatter (SSC) measurements. Each measurement was carried out on ≥ 10,000 cells. In each experiment, freshly isolated control and lupus cells were analyzed in parallel. Detailed protocols for assessment of mitochondrial dysfunction in SLE have been recently described [8].

Microarray analysis of gene expression. RNA was extracted from Jurkat cells carrying doxycycline-inducible GFP-producing control, HRES-1/Rab4 and GFP-producing expression vector (HRES-1/Rab4), or dominant- negative HRES-1/$Rab4^{S27N}$ and GFP-producing expression vector after incubation with or without doxycycline for 24 h (HRES-1/Rab4-DN). Biotinylated cRNA was produced by in vitro transcription and hybridized to Affymetrix HG-U133 Plus-2

chips with 54,675 probe sets, as earlier described [9;10]. Log2-based normalized data were evaluated for opposing doxycycline-induced changes in gene expression in cells expressing HRES-1/Rab4 versus HRES-1/Rab4^{S27N} at 99.99% confidence interval. Fold changes relative to the mean were displayed in heat diagrams [11]. Pathway analysis was performed using Strings 9.0 protein-protein interaction predictor software (http://string-db.org) and false discovery rate (FDR) p values were determined with Bonferrroni correction.

Western blot analyses. Whole cell protein lysates were prepared by lysis in radio-immunoprecipitation assay buffer (150 mM NaCl, 2% NP-40, 0.5% sodium deoxycholate, 0.1% SDS, 50 mM Tris pH 8.0, 1 mM PMSF, 1 μg/ml aproptinin, 1 μg/ml pepstatin, 1 μg/ml leupeptin, 1 mM NaF, 1 mM sodium orthovanadate, 0.1 mM sodium molybdate, 10 mM sodium pyrophosphate) at a density of 4 x 10^7 cells/ml on ice, followed by addition of equal volumes of Laemmli protein sample buffer (60 mM Tris-Cl pH 6.8, 2% SDS, 10% glycerol, 5% β-mercaptoethanol, 0.01% bromophenol blue) and heated to 95°C for 5 minutes prior to separation on SDS-PAGE gels and transfer to 0.45 μm nitrocellulose membranes. HRES-1/Rab4 was detected by primary rabbit antibodies directed to the C-terminus (Santa Cruz sc-312) and Ab 13407 directed to full-length native protein [12]. Expression of HRES-1/Rab4$^{1-121}$ was detected by G1432 rabbit antibody directed to peptide residues 100-121 (Genemed, San Antonio, TX). Rab4B was detected with mouse monoclonal IgM antibody (sc-271982) and goat polyclonal IgG antibody (Santa Cruz cat # sc-26565). We found dominant expression on the protein level of the full-length 218-amino-acid-long HRES-1/Rab4 coding gene in human lymphocytes [12] and the synthenic Rab4A gene in mouse lymphocytes, respectively; GenBank™ accession number AY585832. All expression and gene transduction data on HRES-1/Rab4 in this paper refer to this gene product.

mTOR (#2972), phospho-mTOR (Ser 2448, #2971), 4E-BP1 (#9644), phospho-4E-BP1 (Thr 37/46, #2855), pan-Akt (#4685), phospho-Akt (Ser 473, #4058), phospho-Drp1 (Ser 637, #6319), TSC1 (#4906), TSC2 (#3990), Raptor (#2280), mLST8 (#3274), LC3A/B (#4108), and LC3B (#2775) antibodies were obtained from Cell Signaling. Rab4A (sc-312), Drp1 (sc-32898), p70 S6 kinase (sc-8418), phospho-p70 S6 kinase (Thr 389, sc-8416), and Beclin-1 (sc-11427) antibodies were from Santa Cruz Biotechnology. Rictor antibody (#A500-002A) was from Bethyl laboratories. VDAC1 (ab61273) and Rab5 (ab18211) antibodies were from Abcam. AKAP10 antibody (NBP1-56509) was from Novus Biologicals. Antibodies to human and mouse TCR/CD3ζ (sc-1239) and mouse CD4 (sc-7219) were obtained from Santa Cruz. Human CD4 was detected with monoclonal mouse antibody 4B12 from Novocastra/Leica (NCL-L-CD4-368). Reactivities to primary antibodies were detected with horseradish peroxidase-conjugated secondary antibodies (Jackson, West Grove, PA) and visualized by enhanced chemiluminescence (Western Lightning Chemiluminescence Reagent Plus, GE Health Care/PerkinElmer Life Sciences, Inc., Boston, Massachusetts). Automated densitometry was used to quantify the relative levels of protein expression using a Kodak Image Station 440CF with Kodak 1D Image Analysis Software (Eastman Kodak Company, Rochester, NY).

Confocal microscopy. Lysosomal compartments were labeled by incubating cells at 37°C with 5uM LysoTracker Red (excitation: 577 nm, emission: 590 nm, Invitrogen cat #: L7528) for 30 minutes in complete RPMI. Mitochondria were visualized by staining with 100 nM MitoTracker Deep Red (MTDR, excitation: 644 nm, emission: 665 nm, Invitrogen cat#: M22426). Cells were washed twice and resuspended in 37°C RPMI and allowed to adhere to positively charged

coverslips for 10 minutes, followed by fixation in 4% paraformaldehyde-phosphate buffered saline solution. Visualization of the specimens on the slides was carried out under a Zeiss 510 LSM Meta confocal microscope using Zeiss LSM Image Browser software version 4.2 (Carl Zeiss Microimaging, Thornwood, NJ).

Autophagy induction. Autophagy was induced by treatment with 50 nM rapamycin in the presence and absence of lysosomal inhibitors (200 nM bafilomycin A1, 500 nM folimycin, or 100 μM chloroquine), or protease inhibitors (10 μg/ml leupeptin, 10 μg/ml pepstatin A, or 10 μg/ml E64d) [13]. Autophagy was evaluated in PBL from healthy controls, SLE patients treated without or with rapamycin *in vivo* after stimulation with plate-bound CD3 and soluble CD28 antibodies for 7 days with 200 nM bafilomycin A1 added for lysosomal blockade in the last 24 hours.

Transduction of HRES-1/Rab4 by adeno-associated virus (AAV). HRES-1/Rab4 cDNA was cloned upstream of the internal ribosomal entry site (IRES) sequence in pAAV-IRES-GFP vector (Stratagene, La Jolla, CA) as described previously [12]. Replication-defective virus was produced by co-transfection of AAV-293 cells with control or HRES-1/Rab4 containing pAAV-IRES-GFP vector, pAAV-RC, and pHelper plasmids, 30 μg of each plasmid. Calcium phosphate precipitation was used for transfection, in which 0.3M calcium chloride and 2X HBS solution (NaCl, Na_2HPO_4, HEPES pH 7.1) were added to 90 μg of plasmid DNAs, mixed by bubbling through a Pasteur pipette, and added drop-wise to AAV-293 cells plated in T-175 flasks at 70-80% confluency. Culture medium was replaced 6 hours post-transfection and cells were incubated at 37°C in 5% CO_2.

Virus was collected, filtered, and concentrated 72 h post-transfection. AAV-293 cells and culture medium were transferred to polypropylene tubes through scraping flasks with a rubber policeman. Four freeze-thaw cycles were used to release cell-associated virions by transferring samples from dry ice-100% ethanol to a 37°C water bath. Cellular debris was pelleted by centrifugation in a Sorvall RC-5B refrigerated superspeed centrifuge (Du Pont Instruments, Wilmington, DE) at 10,000 x g for 20 min at 4°C. Supernatants were filtered twice through 5 μm and 0.8 μm Millex SV syringe filters and layered onto 15 ml of Amicon Ultrafree CL centrifugal filter units (Millipore Cat No. UFC4BHK25, Burlington, MA). Samples were centrifuged in a Beckman Allegra 6KR centrifuge (Beckman-Coulter, Indianapolis, IN) at 5000 x g for 30 minutes at room temperature to concentrate viral supernatants. Concentrated virus preparations were frozen at -80°C until use.

Concentrated AAV supernatants were used to infect PBL from healthy controls, SLE patients, and negatively-isolated mouse T cells for 24-48 hours. GFP expression was measured by flow cytometry and equilibrated among constructs. (excitation: 488 nm, emission: 509 nm; FL1 channel). Optimal GFP expression occurred at 48 h post infection of PBL with >99% of cells infected. Mouse T cells were analyzed 24 h post infection, due to a decline in cell viability at 48 h. Over-expression of HRES-1/Rab4 by AAV transduction was confirmed by western blotting using antibody directed to the C-terminus of Rab4A (Santa Cruz, catalog #sc-312).

In vitro prenylation assay. Prenylation of HRES-1/Rab4 and Rab5 was evaluated by western blot analysis of soluble and insoluble fractions from Triton X 114-treated Jurkat cell extracts, as earlier described [14]. Triton X-114 separates hydrophilic proteins from amphiphilic proteins so that lipophilic prenylated Rabs partition to the detergent-rich phase, while unprenylated Rabs

remain in the aqueous phase. Jurkat 6678 cells transfected with wild-type HRES-1/Rab4 and induced with doxycycline for 24 hours in the absence or presence of 500 μM 3-PEHPC or 2 mM 3-PEHPC at 37°C at a cell density of 0.5 million cells/ml. Cells were washed by centrifugation at 1,000 x g in PBS and pellets were lysed in Triton X-114 buffer (20 mM Tris, 150 mM NaCl, 1% Triton X-114, pH 7.5). Lysates were cleared by centrifugation at 13,000 x g for 15 minutes. The supernatant was then incubated at 37°C for 10 minutes, followed by centrifugation at 13,000 x g for 2 minutes. The aqueous supernatant was used as cytosolic compartment. Equal volume of lysis buffer without Triton X-114 (20 mM Tris, 150 mM NaCl, pH 7.5) was added to the detergent-rich membrane phase to replace the aqueous supernatant. ¼ volume of Laemmli buffer was added to the cytosolic and membranous phases before analysis by SDS-PAGE gels and western blotting.

Disease monitoring in MRL/lpr mice. Development of nephritis was monitored in MRL/lpr mice by measurement of proteinuria every 2 weeks starting at 4 weeks of age until the end of the study at 14 weeks of age. Urine was collected from the bottom of cages after housing mice in individual cages without bedding for 4 hours. Urine protein was measured by Bradford protein assay (Bio-Rad, catalog #500-006) using 2 μl of urine. Proteinuria and glucosuria were also measured using Chemstrip 10 (Roche, catalog #1 1895362160). In parallel, serum was collected by submandibular bleeding for measurement anti-nuclear auto-antibodies (ANA). To assess for potential treatment toxicities, mice were weighed weekly.

ELISAs for assays antinuclear antibody (ANA) and cytokine production. ANA was measured in 2 μl of serum by ELISA using manufacturer's protocol (Alpha Diagnostics International; catalog # 5210). Results were read on a Biotek Synergy II plate reader equipped with Gen5 software at absorbances of 450 nm and 630 nm, with the 630 nm subtracted from the 450 nm measurement for background reduction.

IFN-γ, IL-10, and IL-17A were measured in 25 μl of serum using BioLegend Max ELISA kit according to the manufacturer's protocols (IFN- γ, catalog #430807; IL-10, catalog #431407; IL-17A, catalog # 432507). Cytokine ELISAs were performed in duplicates averaged for each mouse prior to statistical analysis. Results were read on a Biotek Synergy II plate reader equipped with Gen5 software at absorbance of 450 nm and 570 nm, with the 570 nm subtracted from the 450 nm measurement for background reduction. For ANA and cytokine ELISAs, a standard curve was prepared for each assay and absorbance values were converted into U/mL or pg/mL by linear regression using GraphPad Prism 5.0 software.

Renal pathology. At the time of sacrifice, a kidney was removed from each mouse and transferred into 10% formalin. Samples were paraffin-embedded, sectioned, and stained with Periodic Acid-Schiff (PAS) and hematoxylin. Histology was assessed by scoring for glomerulonephritis (GN), glomerulosclerosis (GS), interstitial nephritis (IN) on a 0-4 scale, as well as determining the percentage of sclerotic and crescentric glomeruli [15;16]. Slides were scored independently by expert pathologists blinded to the treatment groups.

Treatment of mice with Rab geranylgeranyl transferase inhibitor 3-PEHPC and rapamycin. Twenty-four female MRL/lpr mice were separated into four treatment groups: 4 mice were treated with PBS (solvent control for 3-PEHPC), 4 were treated with 0.2% carboxymethylcellulose (CMC, solvent control for rapamycin), 8 were treated with 125 μg/kg 3-

PEHPC in PBS, and 8 were treated with 1 mg/kg rapamycin in CMC. PBS and 3-PEHPC were injected subcutaneously. CMC and rapamycin were injected intraperitoneally in the left lower quadrant of the abdomen 3 times a week. 3-PEHPC was prepared in PBS, filter-sterilized, and stored in aliquots at 4°C until use. Rapamycin solution was prepared freshly on each date by dissolving rapamycin stock solution (prepared in DMSO) in 0.2% CMC warmed to 37°C and mixed thoroughly by vortexing. Rapamycin solution is an emulsion that precipitates out of solution when cooled, so the solution was prepared immediately before injection. Mice were treated for a total of 10 weeks, starting at 4 weeks of age.

Transfection of siRNA. HeLa cells were transfected at 30% confluence in 6-well plates with 200 nM siRNA specific for HRES-1/Rab4 nucleotides 377-399 or scrambled siRNA using the Oligofectamine protocol (Invitrogen/Life Technologies, Gaithersburg, MD). Jurkat cells or primary lymphocytes can only be transfected by siRNA using electroporation, resulting in significant (>50%) loss of viability and altered mitochondrial homeostasis. Therefore, we utilized HeLa cells which can be transfected with siRNA without change in viability using Oligofectamine Transfection Reagent (Invitrogen/Life Technologies). All siRNAs were synthesized with an Alexa-647 tag by Qiagen and delivery regularly exceeding 95% was monitored by flow cytometry. Gene expression was assayed by western blot 48h after transfection.

Statistical analysis. Statistical analyses were performed using Statview 5.0.1 (SAS Institute, Cary, NC) and GraphPad Prism 5.0 Software (San Diego, CA). Data were expressed as the mean ± standard error of the mean (SEM) of individual experiments. Pair-wise repeated measures analysis of variance (ANOVA), two-way ANOVA, and Student's t-tests were used for analysis of results. Changes were considered significant at p value < 0.05.

LEGENDS TO SUPPLEMENTARY FIGURES S1-S7

Fig. S1. Effect of wild-type HRES-1/Rab4 and dominant-negative HRES-1/Rab4^{S27N} (HRES-1/Rab4-DN) on accumulation of mitochondria, detected with MitoTracker Deep Red (MTDR), and on the co-localization of mitochondria with lysosomes, detected with LysoTracker Red (LTR). A, Immunofluorescence microscopy of Jurkat cells carrying doxycycline-inducible GFP-producing control (Control), HRES-1/Rab4 and GFP-producing expression vector (HRES-1/Rab4), or dominant- negative HRES-1/Rab4^{S27N} and GFP-producing expression vector (HRES-1/Rab4-DN) were pre-incubated in the presence (+D) or absence of doxycycline for 24 h and analyzed by confocal microscopy. B, Cumulative analysis of mitochondrial mass (MTDR) lysosomal mass (LTR) and their colocalization using the NIH Image J software. Data represent mean ± SE of 35 to 79 cells per parameter.

Fig. S2. Effect of wild-type HRES-1/Rab4 and dominant-negative HRES-1/Rab4^{S27N} (HRES-1/Rab4-DN) on LC3-I and LC3-II protein levels in Jurkat cells carrying doxycycline-inducible GFP-producing control expression vector (Control), HRES-1/Rab4 and GFP-producing expression vector (HRES-1/Rab4), or dominant-negative HRES-1/Rab4^{S27N} and GFP-producing expression vector (HRES-1/Rab4-DN). A, Endogenous LC3 was assessed by western blot analysis in cells cultured in the presence of 200 nM bafilomycin A1, in the presence (+D) or absence of doxycycline, without or with 50 nM rapamycin for 24 h. Cumulative data represent 4 independent experiments. B, Processing of exogenous LC3 was assessed 48 h after infection with AAV expressing FP650-LC3 fusion protein. Cells were cultured in the presence or absence of 200 nM Bafi for 24 h before extracting protein lysates for western blot analysis. Representative western blot (top panel) and cumulative analysis of 4 independent experiments (bottom panel) are shown. p values < 0.05 reflect two-tailed paired t-tests.

Fig. S3. Increased expression of Rab4A and depletion of Drp1 in lupus-prone mice. A, Western blot analysis of Rab4A expression in 4-week-old lupus-prone NZB x NZW F1 (NZB/W F1) female mice in comparison to age-matched NZW/LacJ (NZW) and C57BL/6 (B6) female controls. Protein lysates were prepared from un-fractionated splenocytes, T cells, macrophages, or thymocytes, as indicated. 4-month-old (4M) disease-free NZB/W F1 and B6.NZMSle1.Sle2.Sle3 were also analyzed. Data represent mean ± SE of 6-8 mice per strain. B, Western blot analysis of Rab5 expression in 4-week-old NZB/W F1 female mice in comparison to age-matched NZW and B6 female controls as well as in 4-month-old (4M) NZB/W F1 and B6 controls. C, Western blot analysis of CD3ζ and CD4 protein levels in 4-week-old and 4-month-old (4M) NZB/W F1 as well as NZW and B6 control mice. D, Western blot analysis of Beclin 1 in 4-week-old NZB/W F1 as well as NZW and B6 control mice. E, NO production in splenocyte subsets of 4-week-old NZB/W F1 lupus-prone mice as well as age-matched NZW and B6 control mice. NO was measured by DAF-FM fluorescence using flow cytometry and expressed as mean fluorescence intensity (MFI) relative to B6 control mice normalized to 1.0 for each cell type. Data represent mean ± SE in 8 mice per strain. p values reflect comparison to B6 controls.

Fig. S4. Assessment of mTOR activity via phosphorylation and expression of its substrates S6K and 4E-BP1 in 4-week-old female NZB/NZW F1 mice and NZW as well as B6 control mice. mTOR activity was also evaluated in 4-month-old (4M) and 6-month-old NZB/NZW F1 mice

(6M) relative to 4-month-old B6 mice. For each parameter 4 or more mice were analyzed; p values < 0.05 are indicated.

Fig. S5. Effect of aging on mitochondrial homeostasis evaluated by NO production (DAF-FM fluorescence), mitochondrial transmembrane potential ($\Delta\Psi_m$, $DiOC_6$ and TMRM fluorescence), and mitochondrial mass (MTG fluorescence) in mouse splenocytes using flow cytometry. A, Assessment of aging on mitochondrial homeostasis in B6 mice at ages of 3 months (B6 3M), 8 months (B6 8M) and 12 months (B6 12M). Data represent mean ± SE in 4-8 mice per group. p values < 0.05 are indicated. B, 6-month-old (NZB/W F1 6M) and 11-month-old NZB/W F1 lupus prone mice (NZB/W F1 11M) were evaluated relative to 6-month-old NZW controls (NZW 6M). C, Western blot detection of VDAC relative to β-actin in splenocytes of 6-month-old NZB/W F1 lupus prone mice (NZB/W F1) and age-matched B6 and NZW controls. Bar charts reflect cumulative analysis of 4-6 mice per group; $p < 0.05$ is indicated.

Fig. S6. Influence of 3-PEHPC on partitioning of HRES-1/Rab4 and Rab5 to the cytosol. Jurkat cells were incubated without or with 0.5 mM or 2.0 mM 3-PEHPC for 24 h. HRES-1/Rab4 and Rab5 protein levels relative to β-actin were analyzed by western blot of cytosolic and membrane fractions. Representative western blot (left) and mean ± SE two independent experiments are shown (right panel).

Fig. S7. Schematic model for inhibition of mitophagy and accumulation of mitochondria in lupus T cells. A, Regulation of autophagy and mTOR pathways by HRES-1/Rab4. Overall stimulation of autophagy by HRES-1/Rab4 is indicated by the enhanced lipidation of LC3, resulting in lysosomal degradation of CD4, CD3ζ, and Drp1. In the absence of Drp1, mitophagy is inhibited, resulting in the accumulation of mitochondria. B, Molecular hierarchy of metabolic checkpoints that control increased T-cell activation through the accumulation of mitochondria and reorganization of the supramolecular activating complex (SMAC) in SLE. NO induces expression of HRES-1/Rab4 and positive feedback amplification of mTORC1, causing 1) mTORC1-dependent (rapamycin-inhibited) enhancement of recycling and degradation of CD3ζ and CD4 and 2) mTORC1-independent (rapamycin-resistant) but Rab geranylgeranyl transferase-dependent (3-PEHPC-inhibited) degradation of Drp1 and accumulation of mitochondria. Color coding, blue: molecules; green: pathways.

REFERENCES

(1) Tan EM, Cohen AS, Fries JF, Masi AT, McShane DJ, Rothfield NF et al. The 1982 revised criteria for the classification of systemic lupus erythematosus. Arth Rheum 1982; 25:1271-1277.

(2) Hochberg MC. Updating the American College of Rheumatology revised criteria for the classification of systemic lupus erythematosus. Arth Rheum 1997; 40(9):1725.

(3) Bombardier C, Gladman DD, Urowitz MB, Caron D, Chang CH, the committee on prognosis studies in SLE. Derivation of the SLEDAI. A disease activity index for lupus patients. Arth Rheum 1992; 35:630-640.

(4) Perl A, Gonzalez-Cabello R, Lang I, Gergely P. Effector activity of OKT4+ and OKT8+ T-cell subsets in lectin- dependent cell-mediated cytotoxicity against adherent HEp-2 cells. Cell Immunol 1984; 84:185-193.

(5) Ishihara N, Nomura M, Jofuku A, Kato H, Suzuki SO, Masuda K et al. Mitochondrial fission factor Drp1 is essential for embryonic development and synapse formation in mice. Nat Cell Biol 2009; 11(8):958-966.

(6) Banki K, Hutter E, Gonchoroff N, Perl A. Elevation of mitochondrial transmembrane potential and reactive oxygen intermediate levels are early events and occur independently from activation of caspases in Fas signaling. J Immunol 1999; 162:1466-1479.

(7) Nagy G, Koncz A, Perl A. T cell activation-induced mitochondrial hyperpolarization is mediated by Ca^{2+}- and redox-dependent production of nitric oxide . J Immunol 2003; 171:5188-5197.

(8) Perl A, Hanczko R, Doherty E. Assessment of mitochondrial dysfunction in lymphocytes of patients with systemic lupus erythematosus. In: Perl A, editor. Meth. Mol.Med. Autoimmunity: Methods and Protocols. 2 ed. Clifton,NJ: Springer; 2012. 61-89.

(9) Hanczko R, Fernandez D, Doherty E, Qian Y, Vas Gy, Niland B et al. Prevention of hepatocarcinogenesis and acetaminophen-induced liver failure in transaldolase-deficient mice by N-acetylcysteine. J Clin Invest 2009; 119:1546-1557.

(10) Fernandez DR, Telarico T, Bonilla E, Li Q, Banerjee S, Middleton FA et al. Activation of mTOR controls the loss of TCRζ in lupus T cells through HRES-1/Rab4-regulated lysosomal degradation. J Immunol 2009; 182:2063-2073.

(11) Saeed AI, Sharov V, White J, Li J, Liang W, Bhagabati N et al. TM4: A free, open-source system for microarray data management and analysis. Biotechniques 2003; 34(2):374-378.

(12) Nagy G, Ward J, Mosser DD, Koncz A, Gergely P, Stancato C et al. Regulation of CD4 Expression via Recycling by HRES-1/RAB4 Controls Susceptibility to HIV Infection. J Biol Chem 2006; 281:34574-34591.

(13) Rubinsztein DC, Cuervo AM, Ravikumar B, Sarkar S, Korolchuk VI, Kaushik S et al. In search of an autophagomometer. Autophagy 2009; 5(5):585-589.

(14) Baron RA, Tavare R, Figueiredo AC, Blazewska KM, Kashemirov BA, McKenna CE et al. Phosphonocarboxylates inhibit the second geranylgeranyl addition by Rab geranylgeranyl transferase. J Biol Chem 2009; 284(11):6861-6868.

(15) Passwell J, Schreiner GF, Nonaka M, Beuscher HU, Colten HR. Local extrahepatic expression of complement genes C3, factor B, C2, and C4 is increased in murine lupus nephritis. J Clin Invest 1988; 82(5):1676-1684.

(16) Bao L, Haas M, Pippin J, Wang Y, Miwa T, Chang A et al. Focal and segmental glomerulosclerosis induced in mice lacking decay-accelerating factor in T cells. J Clin Invest 2009; 119(5):1264-1274.

Figure S1

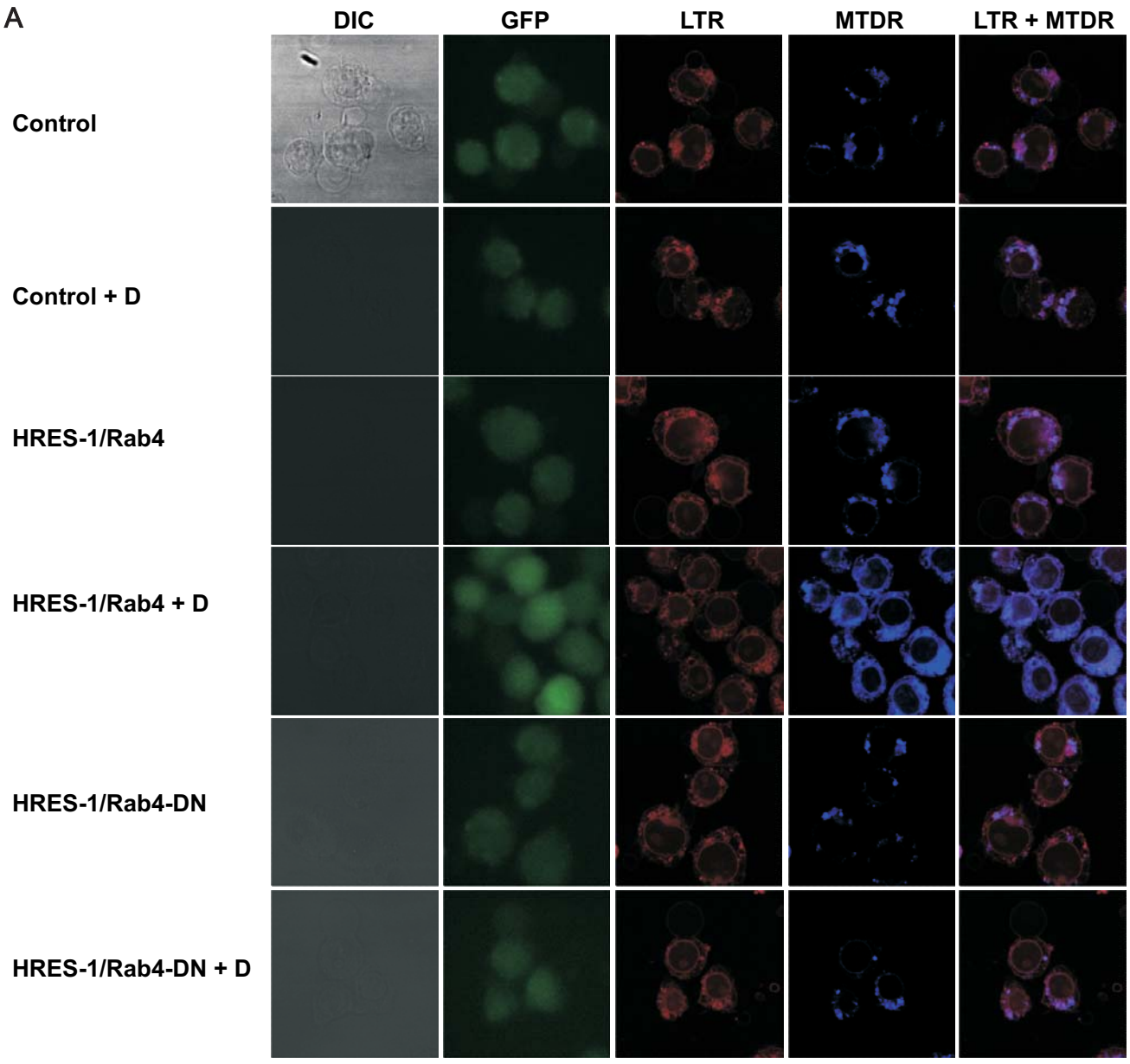
A
DIC
GFP
LTR
MTDR
LTR + MTDR
Control
Control + D
HRES-1/Rab4
HRES-1/Rab4 + D
HRES-1/Rab4-DN
HRES-1/Rab4-DN + D

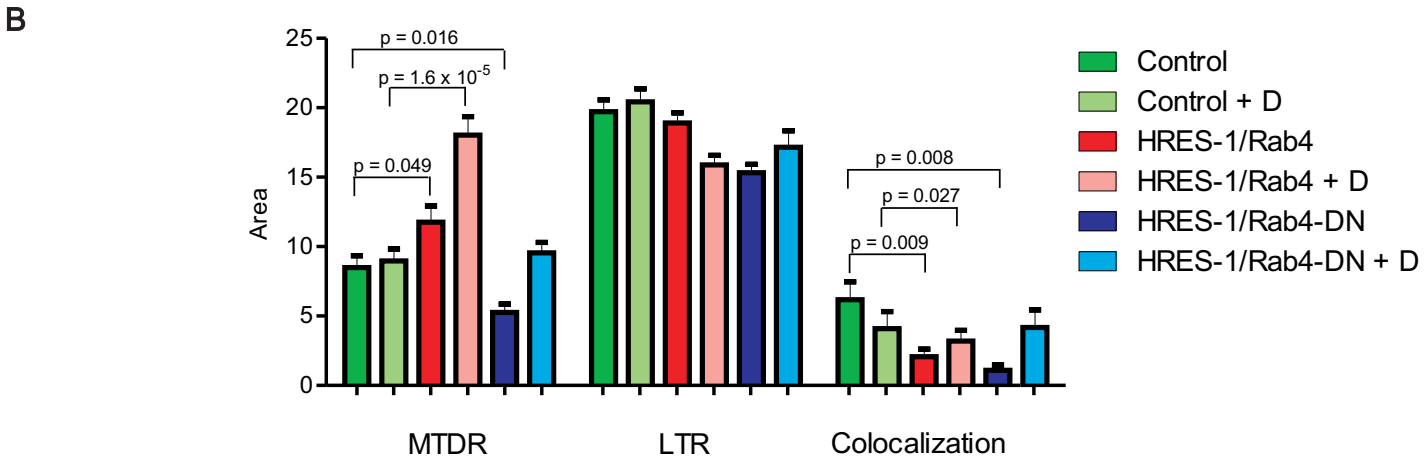
B
Area
25
20
15
10
5
0
p = 0.016
p = 1.6 x 10-5
p = 0.049
p = 0.008
p = 0.027
p = 0.009
MTDR
LTR
Colocalization
Control
Control + D
HRES-1/Rab4
HRES-1/Rab4 + D
HRES-1/Rab4-DN
HRES-1/Rab4-DN + D

Figure S2

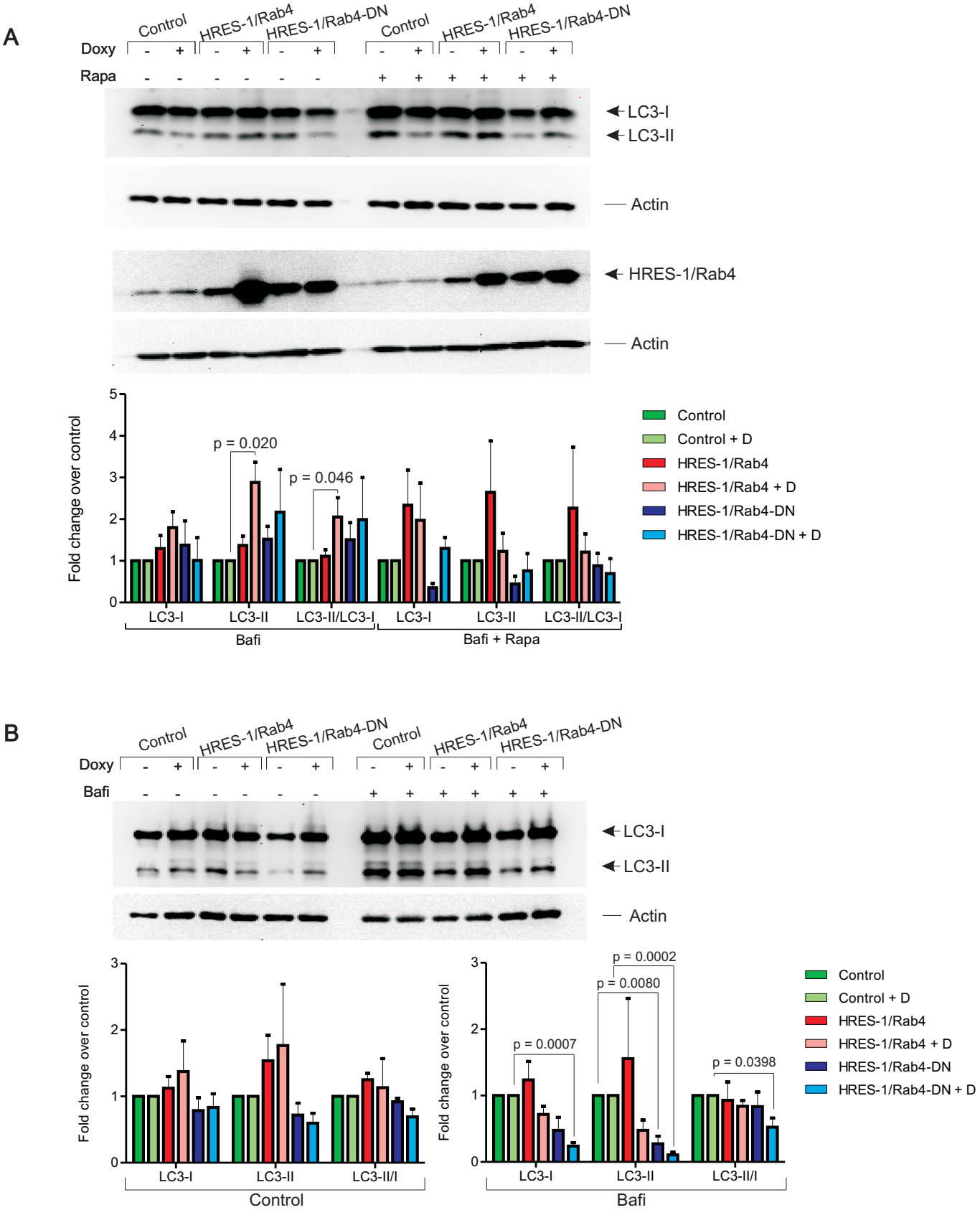
A
Control
HRES-1/Rab4
HRES-1/Rab4-DN
Control
HRES-1/Rab4
HRES-1/Rab4-DN
Doxy
Rapa
LC3-I
LC3-II
Actin
HRES-1/Rab4
Actin
Fold change over control
p = 0.020
p = 0.046
Control
Control + D
HRES-1/Rab4
HRES-1/Rab4 + D
HRES-1/Rab4-DN
HRES-1/Rab4-DN + D
LC3-I
LC3-II
LC3-II/LC3-I
Bafi
Bafi + Rapa
B
Control
HRES-1/Rab4
HRES-1/Rab4-DN
Control
HRES-1/Rab4
HRES-1/Rab4-DN
Doxy
Bafi
LC3-I
LC3-II
Actin
Fold change over control
p = 0.0007
p = 0.0080
p = 0.0002
p = 0.0398
Control
Control + D
HRES-1/Rab4
HRES-1/Rab4 + D
HRES-1/Rab4-DN
HRES-1/Rab4-DN + D
LC3-I
LC3-II
LC3-II/I
Control
Bafi

Figure S3

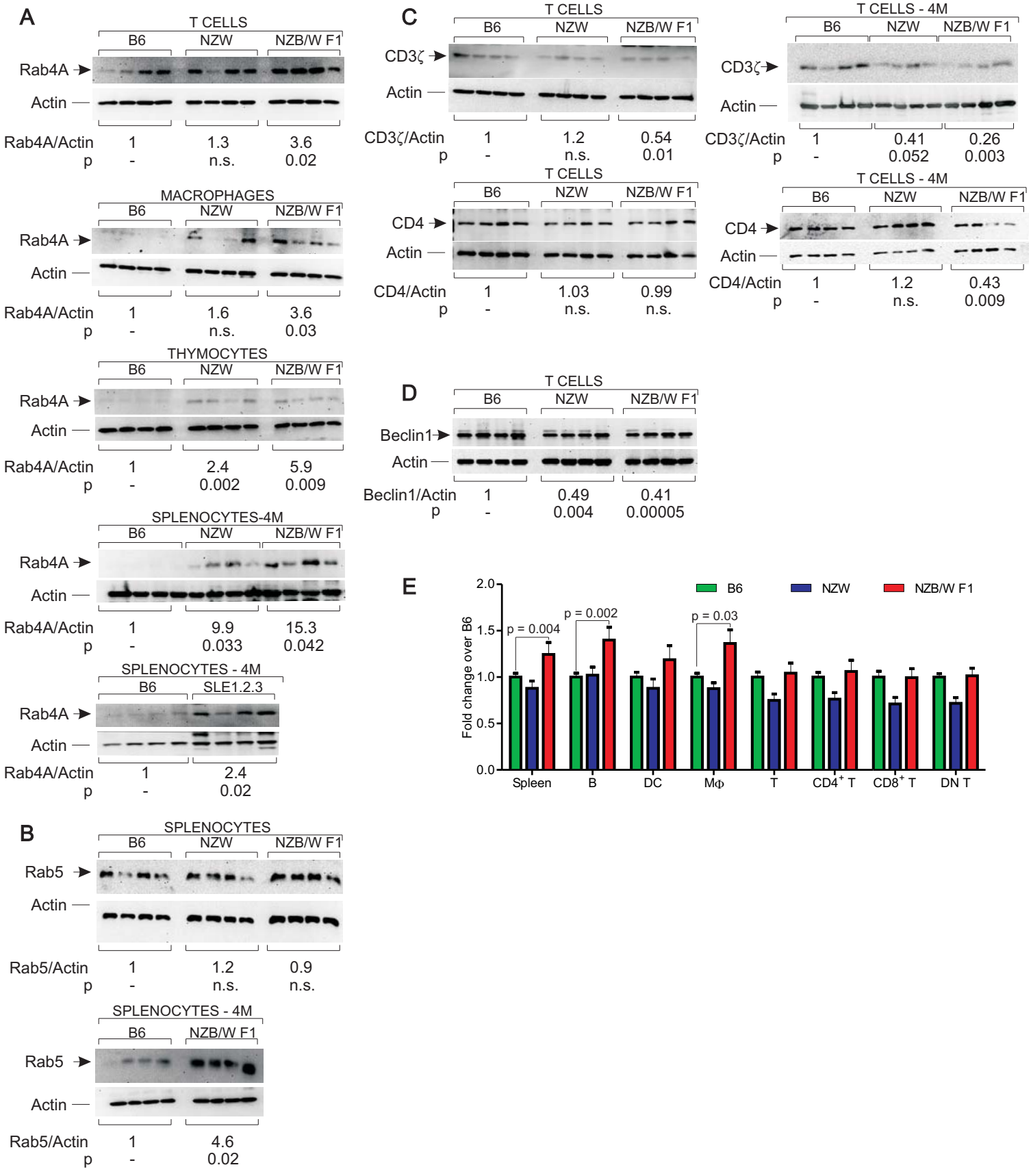
A
T CELLS
B6
NZW
NZB/W F1
Rab4A
Actin
Rab4A/Actin 1 1.3 3.6
p - n.s. 0.02
MACROPHAGES
Rab4A/Actin 1 1.6 3.6
p - n.s. 0.03
THYMOCYTES
Rab4A/Actin 1 2.4 5.9
p - 0.002 0.009
SPLENOCYTES-4M
Rab4A/Actin 1 9.9 15.3
p - 0.033 0.042
SPLENOCYTES - 4M
SLE1.2.3
Rab4A/Actin 1 2.4
p - 0.02
B
SPLENOCYTES
Rab5
Rab5/Actin 1 1.2 0.9
p - n.s. n.s.
SPLENOCYTES - 4M
Rab5/Actin 1 4.6
p - 0.02
C
T CELLS
CD3ζ
CD3ζ/Actin 1 1.2 0.54
p - n.s. 0.01
T CELLS - 4M
CD3ζ/Actin 1 0.41 0.26
p - 0.052 0.003
CD4
CD4/Actin 1 1.03 0.99
p - n.s. n.s.
CD4/Actin 1 1.2 0.43
p - n.s. 0.009
D
Beclin1
Beclin1/Actin 1 0.49 0.41
p - 0.004 0.00005
E
Fold change over B6
p = 0.004
p = 0.002
p = 0.03
Spleen
B
DC
MΦ
T
CD4+ T
CD8+ T
DN T

Figure S4

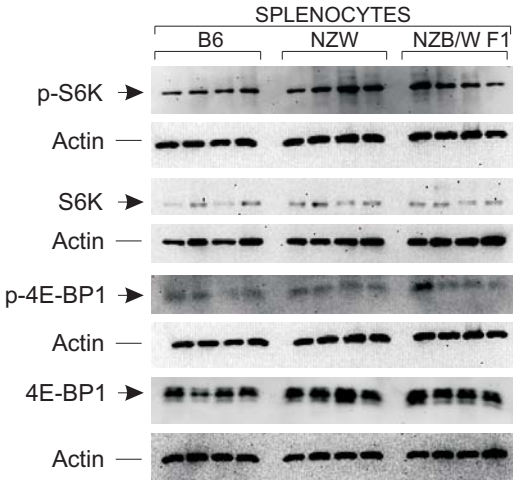
SPLENOCYTES
B6
NZW
NZB/W F1
p-S6K
Actin
S6K
Actin
p-4E-BP1
Actin
4E-BP1
Actin

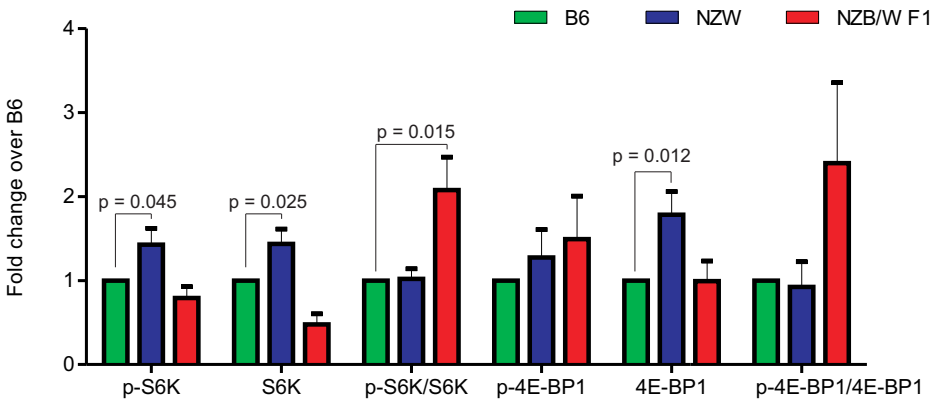
B6
NZW
NZB/W F1
Fold change over B6
p = 0.045
p = 0.025
p = 0.015
p = 0.012
p-S6K
S6K
p-S6K/S6K
p-4E-BP1
4E-BP1
p-4E-BP1/4E-BP1

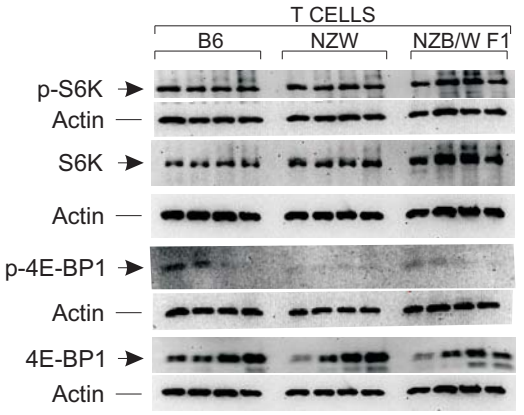
T CELLS
B6
NZW
NZB/W F1
p-S6K
Actin
S6K
Actin
p-4E-BP1
Actin
4E-BP1
Actin

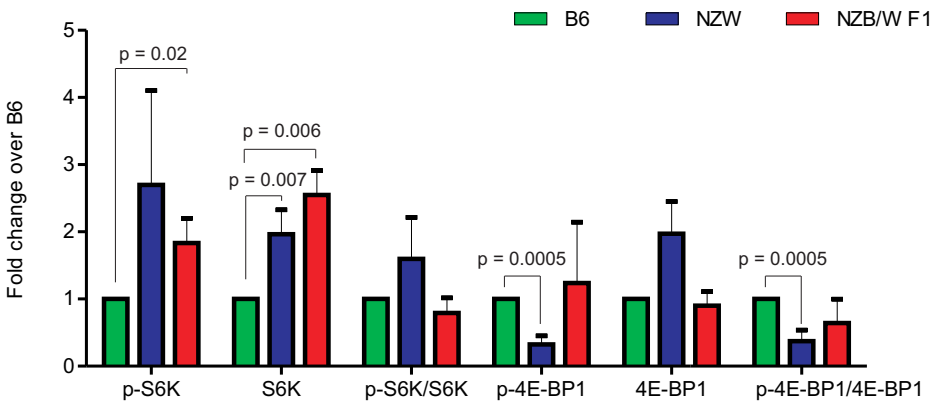
B6
NZW
NZB/W F1
Fold change over B6
p = 0.02
p = 0.006
p = 0.007
p = 0.0005
p = 0.0005
p-S6K
S6K
p-S6K/S6K
p-4E-BP1
4E-BP1
p-4E-BP1/4E-BP1

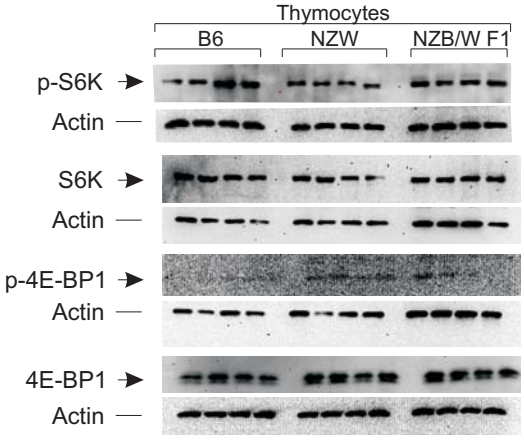
Thymocytes
B6
NZW
NZB/W F1
p-S6K
Actin
S6K
Actin
p-4E-BP1
Actin
4E-BP1
Actin

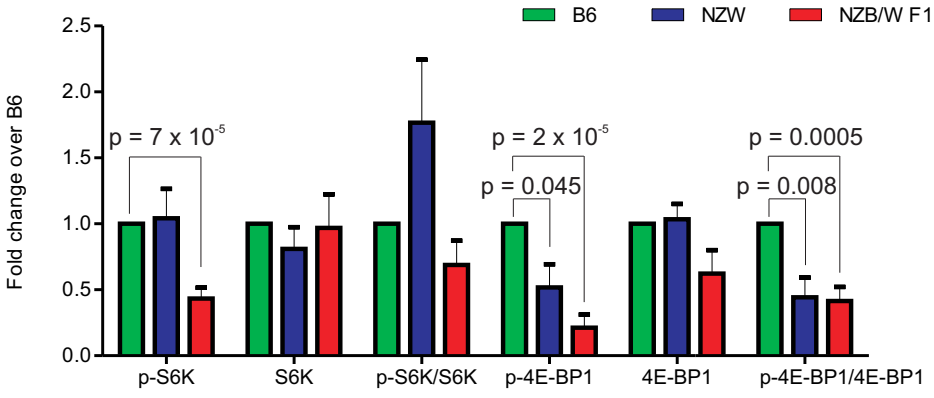
B6
NZW
NZB/W F1
Fold change over B6
p = 7 x 10-5
p = 2 x 10-5
p = 0.0005
p = 0.045
p = 0.008
p-S6K
S6K
p-S6K/S6K
p-4E-BP1
4E-BP1
p-4E-BP1/4E-BP1

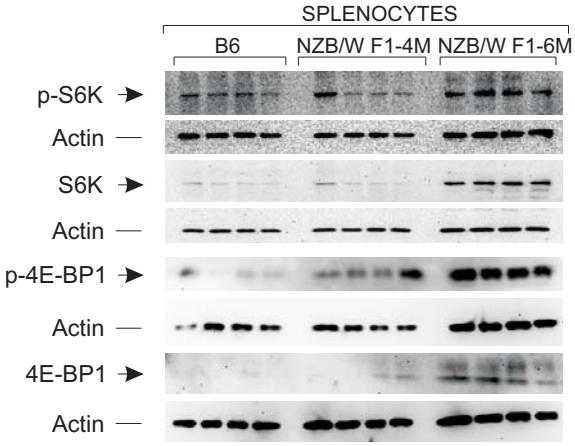
SPLENOCYTES
B6
NZB/W F1-4M
NZB/W F1-6M
p-S6K
Actin
S6K
Actin
p-4E-BP1
Actin
4E-BP1
Actin

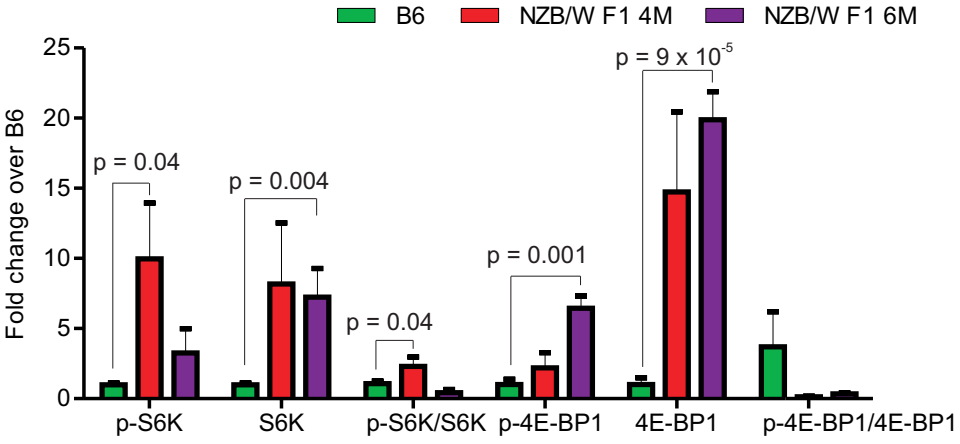
B6
NZB/W F1 4M
NZB/W F1 6M
Fold change over B6
p = 0.04
p = 0.004
p = 0.04
p = 0.001
p = 9 x 10-5
p-S6K
S6K
p-S6K/S6K
p-4E-BP1
4E-BP1
p-4E-BP1/4E-BP1

Figure S5

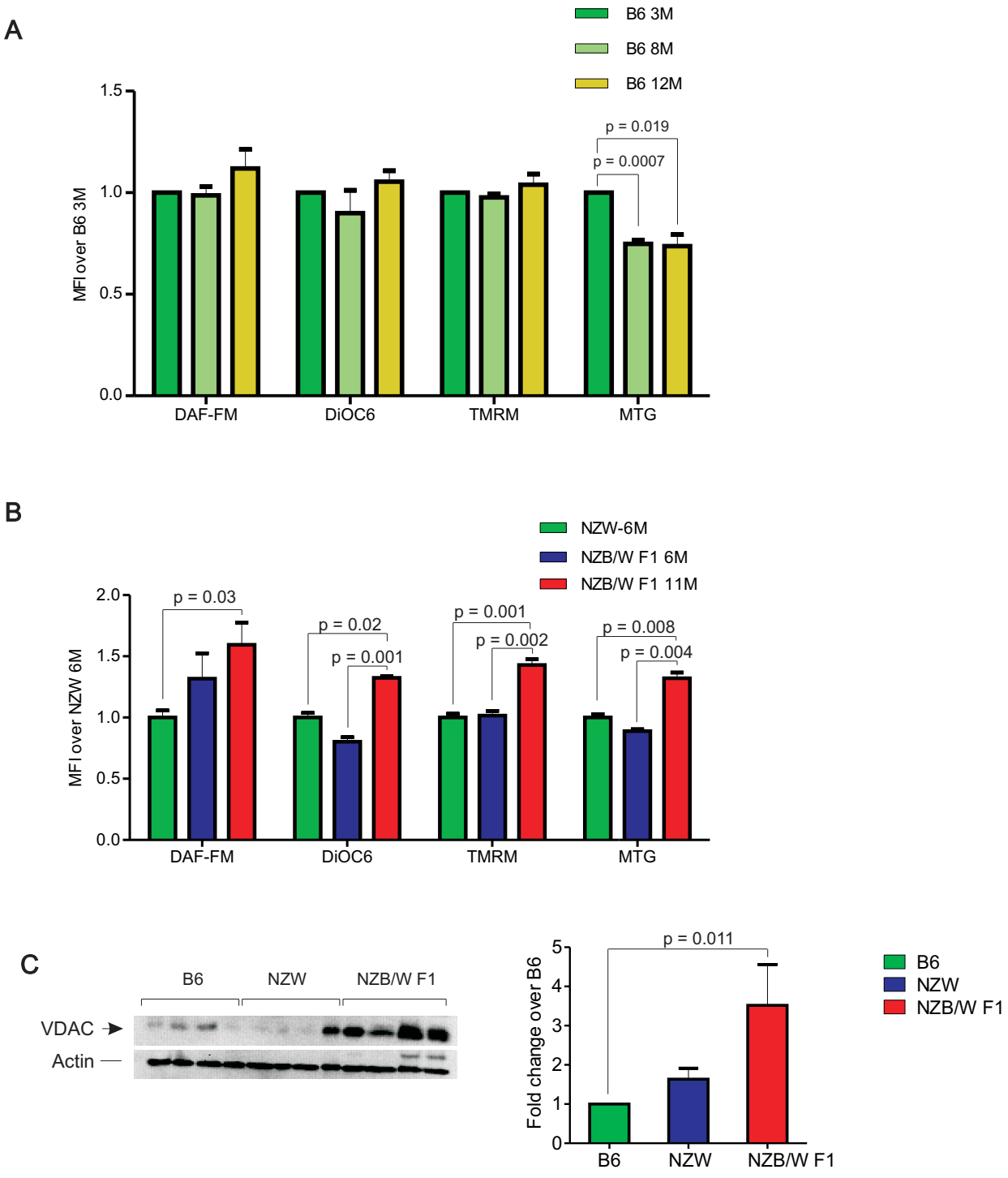
A
B6 3M
B6 8M
B6 12M
MFI over B6 3M
1.5
1.0
0.5
0.0
p = 0.019
p = 0.0007
DAF-FM
DiOC6
TMRM
MTG
B
NZW-6M
NZB/W F1 6M
NZB/W F1 11M
MFI over NZW 6M
2.0
1.5
1.0
0.5
0.0
p = 0.03
p = 0.02
p = 0.001
p = 0.001
p = 0.002
p = 0.008
p = 0.004
DAF-FM
DiOC6
TMRM
MTG
C
B6
NZW
NZB/W F1
VDAC
Actin
p = 0.011
Fold change over B6
5
4
3
2
1
0
B6
NZW
NZB/W F1
B6
NZW
NZB/W F1

Figure S6

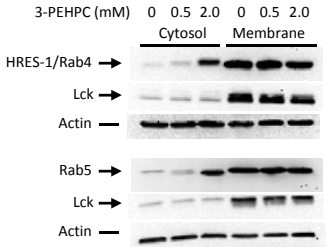
3-PEHPC (mM) 0 0.5 2.0 0 0.5 2.0
Cytosol
Membrane
HRES-1/Rab4
Lck
Actin
Rab5
Lck
Actin

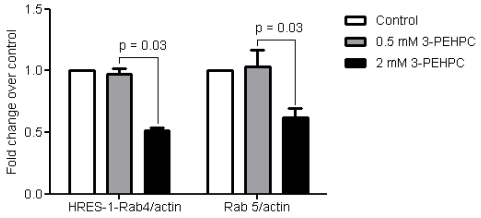
Fold change over control
1.5
1.0
0.5
0.0
p = 0.03
p = 0.03
HRES-1-Rab4/actin
Rab 5/actin
Control
0.5 mM 3-PEHPC
2 mM 3-PEHPC

Figure S7

A

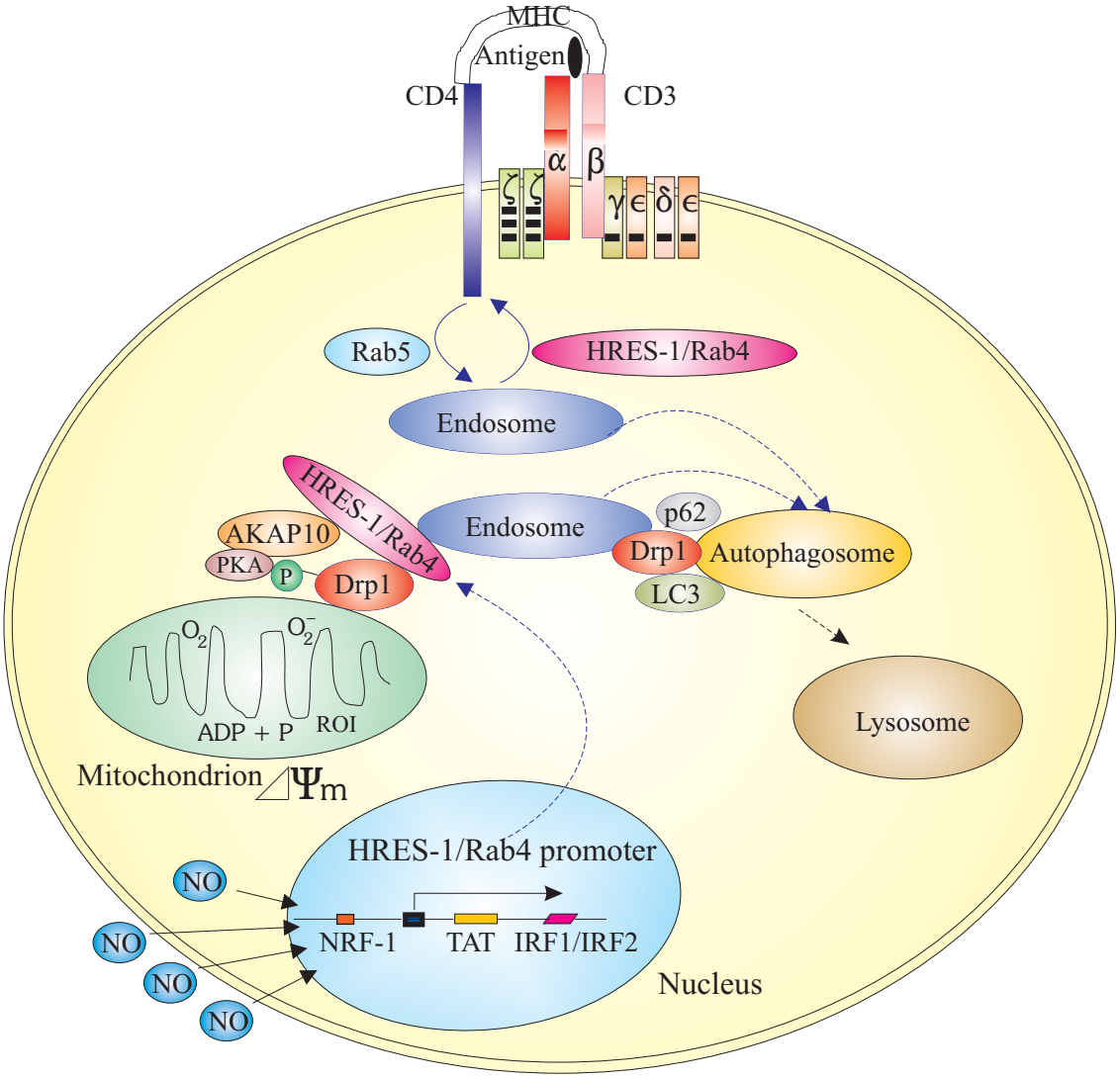
MHC
Antigen
CD4
CD3
α
β
ζ
ζ
γ
ϵ
δ
ϵ
Rab5
HRES-1/Rab4
Endosome
HRES-1/Rab4
AKAP10
PKA
P
Drp1
Endosome
p62
Drp1
Autophagosome
LC3
Lysosome
O2
O2−
ADP + P
ROI
Mitochondrion ΔΨm
HRES-1/Rab4 promoter
NO
NO
NO
NO
NRF-1
TAT
IRF1/IRF2
Nucleus

B

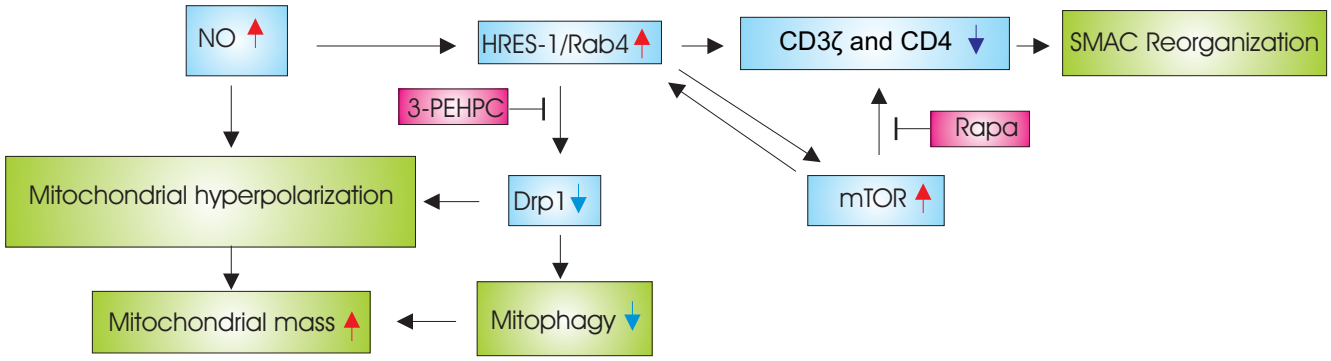
NO
HRES-1/Rab4
CD3ζ and CD4
SMAC Reorganization
3-PEHPC
Rapa
Mitochondrial hyperpolarization
Drp1
mTOR
Mitochondrial mass
Mitophagy